INVESTIGATION OF OPTICAL SPECTRA AND ELECTRON PARAMAGNETIC RESONANCE PARAMETERS FOR Cu^{2+} IONS IN $LiNbO_3$ CRYSTAL

Z.-F. Zhou*, F. Chen, J. Yang

College of Physics and Electronic Information,
Shangrao Normal College, Shangrao Jiangxi, China;
Research Center of Intelligent Engineering Technology of Electronic Vehicle Parts in Jiangxi Province, Shangrao, China

The optical spectrum band positions and electron paramagnetic resonance (EPR) parameters – g factors (g_x, g_y, g_z) and the hyperfine structure constants (A_x, A_y, A_z) for Cu^{2+} doped in $LiNbO_3$ crystal are theoretically investigated using the perturbation formulas of these EPR parameters for a $3d^9$ ion under rhombically elongated octahedra based on the cluster approach. The doped Cu^{2+} was assumed to substitute for the host Li^+ in the lattice, with a different local environment from the original Li^+ due to size mismatch and the Jahn–Teller effect. Based on the calculations, the Cu-O bonds are found to suffer the axial elongation δz (~0.0611 Å) along the z-axis, and the planar bond length experiences an additional variation δr (~0.0861 Å) along the x- and y-axis respectively. Meanwhile, the ground-state wave function for the Cu^{2+} center in $LiNbO_3$ was also obtained.

***Keywords*:** *electron paramagnetic resonance, crystal-field theory, local structure, $LiNbO_3$, Cu^{2+}.*

ОПТИЧЕСКИЕ СПЕКТРЫ И ПАРАМЕТРЫ ЭЛЕКТРОННОГО ПАРАМАГНИТНОГО РЕЗОНАНСА ИОНОВ Cu^{2+} В КРИСТАЛЛЕ $LiNbO_3$

Z.-F. Zhou*, F. Chen, J. Yang

УДК 543.429.22

Колледж физики и электронной информации Шанграо, Цзянси, Шанграо, Китай;
Научно-исследовательский центр интеллектуальных инженерных технологий электронных деталей автомобилей, Шанграо, Цзянси, Шанграо, Китай; e-mail: zifzhou@126.com

(Поступила 28 января 2021)

Исследованы положения полос оптического спектра, параметры электронного парамагнитного резонанса (ЭПР) — g-факторы (g_x, g_y, g_z) и константы сверхтонкой структуры (A_x, A_y, A_z) — для ионов Cu^{2+} в легированном кристалле $LiNbO_3$ с использованием формул для параметров ЭПР $3d^9$-иона в ромбически вытянутых октаэдрах на основе кластерного подхода. Предполагалось, что ион Cu^{2+} заменит основной Li^+ в решетке с отличающимся от исходного Li^+ локальным окружением из-за несоответствия размеров и эффекта Яна–Теллера. Для связи Cu-O имеет место удлинение δz (~0.0611 Å) вдоль оси z и дополнительное изменение δr (~0.0861 Å) в плоскости осей x и y. Получена волновая функция основного состояния центра Cu^{2+} в $LiNbO_3$.

Ключевые слова: *электронный парамагнитный резонанс, теория кристаллического поля, локальная структура, $LiNbO_3$, Cu^{2+}.*

Introduction. $LiNbO_3$ crystal is an important ferroelectric material. This crystal doped with transition metal (TM) and rare earth (RE) ions has been widely studied to achieve unique optical [1, 2], photorefractive [3, 4], luminescence [5], dielectric [6], and structural properties [7, 8]. Usually, these properties can be closely related to the defect structures and electronic states of the doped ions. Electron paramagnetic resonance (EPR) has long been considered one of the most useful tools for obtaining information on the configurations of the incorporated paramagnetic ions and determine the local structure of the doped TM and RE ions [9–12]. In addition, study of the optical absorption can provide the crystal field parameters and structure of energy

levels of the TM ions [13, 14]. Thus, EPR and optical absorption studies were usually carried out to collect the information about the coordination/local site symmetry and bonding nature of the doped TM ions in the host lattice. The Cu^{2+} ion with d^9 electron configuration is one of the most interesting TM ions because it represents a relatively simpler energy level structure (only one ground state and one excited state under ideal octahedral crystal-fields, up to five levels under rhombic symmetry) and gives valuable information about the ground state and the local symmetry of the ion. Four optical spectrum band positions and the EPR parameters (g factors g_i, with $i = x, y, z$, and the hyperfine structure constants A_i) for $LiNbO_3:Cu^{2+}$ have been measured by Yetrosyan et al. [15].

The theoretical investigations of the EPR parameters of Cu^{2+} doped $LiNbO_3$ have been made by Kuang et al. and Zhang and Xiao [16, 17]. However, previous studies focused only on the EPR parameters using the high-order perturbation formulas. However, until now, as a part of the particular interest in this area, the optical spectra of the $[CuO_6]^{10-}$ cluster in $LiNbO_3$ crystal have not been studied, as the analysis of the optical spectra can also provide useful information about electronic states and local structures of the impurities. Thus, further unified studies on the optical and EPR spectra are an imperative requirement. In this work, four *d-d* transition bands and the EPR parameters, as well as the local structure for $LiNbO_3:Cu^{2+}$, are uniformly investigated from the perturbation formulas of these parameters for a $3d^9$ ion in rhombically elongated octahedra. In the calculation formulas, the reasonable local lattice deformations around the impurity of the Cu^{2+} center due to the Jahn–Teller (JT) effect are included, the ligand orbital and spin-orbit coupling (SOC) contributions to the EPR parameters are considered from the cluster approach, and the admixture of *d*-orbitals in the ground state wave function of the Cu^{2+} center is also taken into account.

Calculations. The structure of $LiNbO_3$ has been determined by X-ray and neutron diffraction [18] as a trigonal structure made up of irregular oxygen octahedra piled along the C_3 axis and sharing faces, where Li^+ and Nb^{5+} cations occupy the octahedral sites. The Nb octahedra exhibit two Nb–O distances, namely, $R_1 \approx 1.889$ Å and $R_2 \approx 2.112$ Å, and the Li octahedra are characterized by two metal–oxygen distances (Li–O) of $R_1 \approx 2.068$ Å and $R_2 \approx 2.238$ Å [18]. When the Cu^{2+} ion enters the lattice of $LiNbO_3$, in view of the charge state and ionic radius of Cu^{2+} (0.73 Å) closer to Li^+ (0.76 Å) than to Nb^{5+} (0.64 Å) [19–21], Yetrosyan et al. [15] tentatively assumed that Cu^{2+} substitutes for Li^+ in the $LiNbO_3$ crystal. However, the ground orbital state of d^9 ions, such as Cu^{2+}, at a trigonal octahedral site of crystals is the orbital doublet ^2E_g with a low spin ($S = 1/2$), which is JT unstable in a trigonal symmetry and undergoes a JT distortion to remove the degeneracy [15]. The optical and EPR spectra of $LiNbO_3:Cu^{2+}$ indicated that the local structure of the $[CuO_6]^{10-}$ cluster is not trigonal like the host Li^+ site but a rhombic distortion owing to the electron–phonon coupling between octahedral E_g electronic states and e_g vibrations ($E_g \otimes e_g$ model). As the EPR parameters of the doped paramagnetic ions are sensitive to its defect structure, one can tentatively obtain the defect structure of a paramagnetic impurity center by studying its experimental EPR parameters.

Local structure of the Cu^{2+} center in $LiNbO_3$. As for a Cu^{2+} ion under octahedra, due to the JT effect, two Cu-O bonds along the C_4 axis can be relaxed by some distance Δz; meanwhile, the other four perpendicular bonds may experience a relative variation δr along the *x*- and *y*-axes, transforming the host trigonally distorted LiO_6 octahedra into the local rhombically distorted CuO_6 one (Fig. 1). Then, the local structure around the impurity Cu^{2+} is different from that of the host Li^+ site in the $LiNbO_3$ single crystal due to the JT effect; for simplicity, the local Cu–O bond lengths R_x, R_y, and R_z along the *x*-, *y*- and *z*-axes in the rhombic $[CuO_6]^{10-}$ cluster can be expressed in terms of the reference distance R, the axial distortion Δz, and the planar bond length variation δr as:

$$R_z \approx R + 2\delta z,\ R_x \approx R - \delta z + \delta r,\ R_y \approx R - \delta z - \delta r. \tag{1}$$

Formulas of the EPR parameters for $LiNbO_3:Cu^{2+}$. The ^2D state of a $3d^9$ ion in an octahedral crystal field will be split into a higher triplet $^2T_{2g}$ and a lower doublet ^2E_g. If the site symmetry is lowered to rhombic, its lower orbital doublet ^2E_g would be separated into two singlets $^2A_{1g}(\theta)$ and $^2A_{1g'}(\varepsilon)$, and the higher cubic orbital triplet $^2T_{2g}$ would split into three singlets $^2B_{1g}$ (ζ), $^2B_{2g}$ (η), and $^2B_{3g}$ (ξ) [22, 23]. As the states $^2A_{1g}(\theta)$ and $^2A_{1g}'(\varepsilon)$ belong to the same representation of a rhombic symmetry group, the ground state should be an admixture of both states [24–26], i.e.,

$$\Phi = \alpha|d_{x^2-y^2}\rangle + \beta|d_{3z^2-r^2}\rangle. \tag{2}$$

Here, α and β are the mixing coefficients owing to the rhombic field components, which satisfy the normalization relation:

$$\alpha^2 + \beta^2 = 1. \tag{3}$$

The high-order perturbation formulas of the EPR parameters for rhombically elongated octahedral $3d^9$ cluster can be expressed as [26]:

$$g_x = g_s + \frac{2k'\zeta'(\alpha+\sqrt{3}\beta)^2}{E_4} - \frac{2\alpha k'\zeta\zeta'(\alpha+\sqrt{3}\beta)}{E_2E_4} + \frac{k'\zeta\zeta'(\alpha^2-3\beta^2)}{E_3E_4} - \frac{2\alpha^2 g_s\zeta'^2}{E_2^2} - \frac{g_s\zeta'^2(\alpha-\sqrt{3}\beta)^2}{2E_3^2} + \frac{2\alpha k\zeta'^2(\alpha-\sqrt{3}\beta)}{E_2E_3},$$

$$g_y = g_s + \frac{2k'\zeta'(\alpha-\sqrt{3}\beta)^2}{E_3} - \frac{2\alpha k\zeta\zeta'(\alpha-\sqrt{3}\beta)}{E_2E_3} + \frac{k\zeta\zeta'(\alpha^2-3\beta^2)}{E_3E_4} - \frac{2\alpha^2 g_s\zeta'^2}{E_2^2} - \frac{g_s\zeta'^2(\alpha+\sqrt{3}\beta)^2}{2E_4^2} + \frac{2\alpha k\zeta'^2(\alpha+\sqrt{3}\beta)}{E_2E_4},$$

$$g_z = g_s + \frac{8\alpha^2 k'\zeta'}{E_2} - \frac{2\alpha k'\zeta\zeta'(\alpha-\sqrt{3}\beta)}{E_2E_3} - \frac{2\alpha k'\zeta\zeta'(\alpha+\sqrt{3}\beta)}{E_2E_4} - \frac{g_s\zeta'^2(\alpha-\sqrt{3}\beta)^2}{2E_3^2} - \frac{g_s\zeta'^2(\alpha+\sqrt{3}\beta)^2}{2E_4^2} - \frac{k'\zeta\zeta'(\alpha-3\beta^2)}{E_3E_4},$$

$$A_x = P_0\left[-\kappa + \frac{2N}{7} + (g_x - g_s) - \frac{3}{14}(g_y - g_s)\right],$$

$$A_y = P_0\left[-\kappa + \frac{2N}{7} + (g_y - g_s) - \frac{3}{14}(g_x - g_s)\right], \quad (4)$$

$$A_z = P\left[-\kappa - \frac{4N}{7} + (g_z - g_s) + \frac{3}{14}(g_x - g_s) + \frac{3}{14}(g_y - g_s)\right].$$

Here, g_s (~2.0023) is the spin-only value; ζ (and ζ′) are the SOC coefficients and k (and k') are the orbital reduction factors; P_0 (~388×10^{-4} cm^{-1} [27, 28]) is the dipolar hyperfine structure parameter of a free Cu^{2+} ion, and thus $P \approx NP_0$; κ is the isotropic core polarization constant for the central Cu^{2+} ($3d^9$) ion in crystals. Generally, the core polarization constant κ can be expressed with an empirical formula $\kappa \sim -2\chi/(3r^{-3})$ [27], where χ represents the density of unpaired spins at the nucleus of the Cu^{2+} ion and $\langle r^{-3}\rangle$ is the characteristic of the expectation value of the inverse cube of the $3d$ radial wave function. Using $\langle r^{-3}\rangle \approx 8.252$ a.u. [27] and $\chi \approx -3.12$ a.u. [23] for the Cu^{2+} ion, the value $\kappa \approx 0.23$ may be estimated.

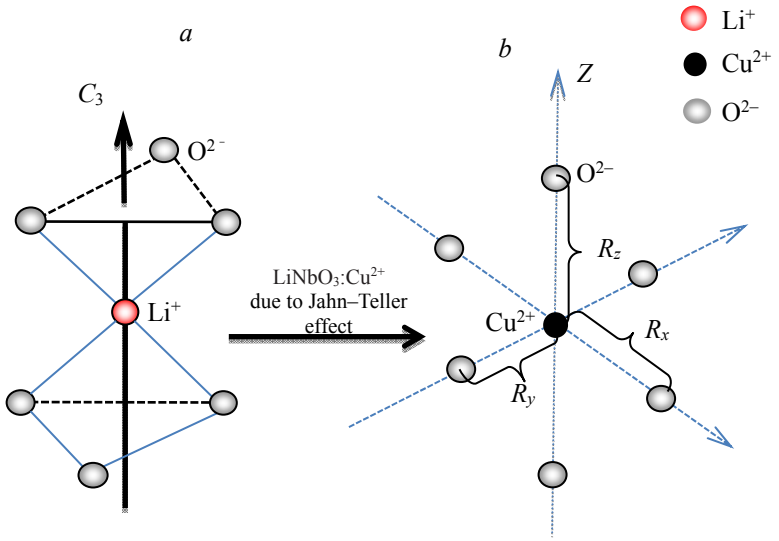

Fig. 1. (a) Structure of the Li^+ site in $LiNbO_3$, (b) the local structure of the impurity Cu^{2+} center in $LiNbO_3$ due to Jahn–Teller effect.

Formulas of the d-d transitions for Cu^{2+} center under rhombic symmetry. In Eq.(3), E_j (j = 1, 2, 3, 4) denote the separations between the excited $^2B_{1g}$, $^2B_{2g}$, $^2B_{3g}$, and $^2A_{1g}$ and the ground $^2A_{1g}'$ states, respectively (Fig. 1). The observed four crystal-field energy levels of a $3d^9$ ion under rhombic symmetry can be described by the crystal-field parameters D_q, D_s, D_t, D_ξ, and D_η:

$$\begin{aligned} E_1 &= -4D - 5D_t, \\ E_2 &= 10D_q, \\ E_3 &= 10D_q - 3D_s + 5D_t - 3D_\xi + 4D_\eta, \\ E_4 &= 10D_q - 3D_s + 5D_t + 3D_\xi - 4D_\eta. \end{aligned} \tag{5}$$

Calculations of the cluster approach. Based on the two SO parameter model, the one-electron basis functions Ψ_γ (where $\gamma = t$ and e represent the irreducible representations T_{2g} and E_g of O_h group) for an octahedral cluster can be given as [29]:

$$\begin{aligned} \Psi_t &= N_t^{1/2}(\phi_t - \lambda_t \chi_{pt}), \\ \Psi_e &= N_e^{1/2}(\phi_e - \lambda_e \chi_{pe} - \lambda_s \chi_s). \end{aligned} \tag{6}$$

Here, φ_γ is the characteristic of the d orbitals of the central ion, whereas $\chi_{p\gamma}$ and χ_s represent the p- and s-orbitals of the ligands. N_γ and λ_γ (or λ_s) are the normalization factors and the orbital admixture coefficients respectively. They can be determined from the normalization conditions:

$$N_t(1 - 2\lambda_t S_{dpt} + \lambda_t^2) = 1 \tag{7}$$

and the approximate relationships:

$$\begin{aligned} N^2 &= N_t^2(1 + \lambda_t^2 S_{dpt}^2 - 2\lambda_t S_{dpt}), \\ N^2 &= N_e^2(1 + \lambda_e^2 S_{dpe}^2 + \lambda_s^2 S_{ds}^2 - 2\lambda_e S_{dpe} - 2\lambda_s S_{ds}), \end{aligned} \tag{8}$$

$S_{dp\gamma}$ (and S_{ds}) are the group overlap integrals. As orbital admixture and overlap between the central ion and ligands have consistent dependence on bond length, one can reasonably adopt the proportional relationship $\lambda_e/S_{dpe} \approx \lambda_s/S_{ds}$ for the same irreducible representation e_g. N is the average covalency factor, characteristic of the covalency effect of the studied system.

Based on the cluster approach [29], the orbital reduction factors k (and k') and the SOC coefficients ζ (and ζ') can be determined as follows:

$$\begin{aligned} \zeta &= N_t(\zeta_d^0 + \lambda_t^2 \zeta_p^0 / 2), \qquad \zeta' = \sqrt{N_t N_e}(\zeta_d^0 - \lambda_t \lambda_e \zeta_p^0 / 2), \\ k &= N_t(1 + \lambda_t^2 / 2), \qquad k' = \sqrt{N_t N_e}[1 - \lambda_t(\lambda_e + \lambda_s A)/2], \end{aligned} \tag{9}$$

where ζ_d^0 (~829 cm^{-1} [30]) and ζ_p^0 (~151 cm^{-1} [27]) are the SOC coefficients of the free Cu^{2+} ($3d^9$) ion and the ligand O^{2-} ions, respectively. A denotes the integral $R\langle ns|\partial/\partial y\rangle np_y$, where R is the reference impurity-ligand distance of the studied system.

Calculations of the optical spectrum band positions and EPR parameters for $LiNbO_3$:Cu^{2+}. For $LiNbO_3$:Cu^{2+}, the rhombic crystal field parameters (D_s, D_t, D_ξ, and D_η) can be determined from the superposition model [31] and local structure of the Cu^{2+} center in $LiNbO_3$:

$$\begin{aligned} D_s &= -\frac{2}{7}\bar{A}_2(R)\left[\left(\frac{R}{R_x}\right)^{t_2} + \left(\frac{R}{R_y}\right)^{t_2} - 2\left(\frac{R}{R_z}\right)^{t_2}\right], \\ D_t &= -\frac{8}{21}\bar{A}_4(R)\left[\left(\frac{R}{R_x}\right)^{t_4} + \left(\frac{R}{R_y}\right)^{t_4} - 2\left(\frac{R}{R_z}\right)^{t_4}\right], \\ D_\xi &= -\frac{2}{7}\bar{A}_2(R)\left[\left(\frac{R}{R_x}\right)^{t_2} - \left(\frac{R}{R_y}\right)^{t_2}\right], \\ D_\eta &= -\frac{10}{21}\bar{A}_4(R)\left[\left(\frac{R}{R_x}\right)^{t_4} - \left(\frac{R}{R_y}\right)^{t_4}\right]. \end{aligned} \tag{10}$$

Here, $t_2 \approx 3$ and $t_4 \approx 5$ are the power-law exponents [32–36]; $\bar{A}_k(R)$ ($k = 2, 4$) are the intrinsic parameters with the reference distance R. For $3d^n$ ions under octahedra, the relationship $\bar{A}_4(R) = 3D_q/4$ and the ratio $\bar{A}_2(R)/\bar{A}_4(R) \approx 10.5$ were proved valid in the previous EPR studies using the superposition model for $3d^n$ ions in many crystals [37, 38], where the cubic crystal-field parameter D_q can be obtained from the experimental optical spectra. From the observed four d-d-transition bands, we have $D_q \approx 870$ cm^{-1}. The covalency factor N can be obtained from the empirical formula $N^2 \approx 1 - h(L)k(M)$ [39]; here, $h(L)$ and $k(M)$ are the characteristics of the ligand and central metal ions, respectively. According to the values $h(O^{2-}) \approx 1$ [39] and $k(Cu^{2+}) \approx 0.3$ [40], $N \approx 0.83$ can be obtained. Using the reference bond length $R = [(R_1 + R_2)/2] \approx 2.155$Å for the host Li^+ site and the SCF functions [41, 42], the group overlap integrals $S_{dpt} \approx 0.0053$, $S_{dpe} \approx 0.0192$, $S_s \approx 0.0153$, and $A \approx 1.4017$ can be calculated. Then, the normalization factors N_γ and the mixing coefficients λ_γ can be calculated from Eqs. (7) and (8). The SOC coefficients ζ (ζ') and the orbital reduction factors k (k') may be determined from Eq. (9). The local impurity-ligand bond distances are received $R_x = 2.180$ Å, $R_y = 2.008$ Å, $R_z = 2.277$ Å along the x, y, and z-axes, respectively; the normalization factors $N_t = 0.831$, $N_e = 0.839$; the orbital admixture coefficients $\lambda_t = 0.456$, $\lambda_e = 0.363$, and $\lambda_s = 0.289$; the spin-orbit coupling coefficients $\zeta = 702.0$ cm^{-1} and $\zeta' = 681.6$ cm^{-1}, and the orbital reduction factors $k = 0.918$ and $k' = 0.688$ for the Cu^{2+} centers in $LiNbO_3$.

Therefore, there are only three parameters (i.e., the mixing coefficient α in the ground-state wave function, the axial bond length elongation δz along the z-axis, and the planar bond length variation δr along the x- and y-axes) are unknown in the above formulas. Substituting these values into Eq. (4) and fitting the calculated EPR parameters to the experimental data, we have:

$$\alpha \approx 0.992, \delta z \approx 0.0611 \text{ Å}, \delta r \approx 0.0861 \text{ Å}, \tag{11}$$

for the copper center. Then, the ground state wave function for $LiNbO_3$:Cu^{2+} can be written as follows:

$$\Phi = 0.992|d_{x^2-y^2}\rangle + 0.126|d_{3z^2-r^2}\rangle. \tag{12}$$

The corresponding calculated optical spectral bands and EPR parameters (Cal. IV) are listed in Table 1. The results (Cal. I) based on the above local structural parameters and the admixture of d-orbitals in the ground-state wave function but neglecting the ligand contributions (i.e., taking $\zeta = \zeta' = N\zeta_d^0$ and $k = k' = N$), and (Cal. II) based on the local structural parameters and including the ligand contributions but neglecting the admixture of d-orbitals (i.e., $\alpha = 1$, $\beta = 0$) in the ground-state wave function and (Cal. III) by the previous works are also collected in Table 1.

TABLE 1. The g Factors g_i ($i = x, y, z$), the Hyperfine Structure Constants A_i (in 10^{-4} cm^{-1}), and the Optical Band Positions (in cm^{-1}) for the Cu^{2+} Center in the $LiNbO_3$ Crystal

Calculation	g_x	g_y	g_z	A_x	A_y	A_z
I	2.118	2.153	2.491	51.3	34.5	−51.2
II	2.060	2.075	2.409	25.8	18.7	−86.7
III	2.175	2.118	2.409	–	–	–
IV	2.095	2.124	2.403	41.9	28.0	−83.1
Experiment [15]	2.095 (5)	2.121 (7)	2.403 (5)	40 (2)	29 (3)	82 (2)

The optical band positions (in cm^{-1}) for the Cu^{2+} center in the $LiNbO_3$ crystal				
$\|d_{x^2-y^2}\rangle \rightarrow$	$\|d_{z^2}\rangle$	$\|d_{xy}\rangle$	$\|d_{xz}\rangle$	$\|d_{yz}\rangle$
Calculation	5013	8670	9598	11.574
Experiment [15]	5000	8700	9600	11.300

N o t e. Calculation I based on the local structural parameters and neglecting the ligand orbit and spin-orbit coupling contributions but the admixture of d-orbitals in the ground-state wave function are taken into account; II based on the local structural parameters and including the ligand orbit and spin-orbit coupling contributions but neglecting the admixture of d-orbitals in the ground-state wave function; III calculated by previous work in Yetrosyan et al. [15]; IV based on the local structural parameters and including the ligand orbit and spin-orbit coupling contributions and the admixture of d-orbitals in the ground-state wave function.

Results and discussion. From Table 1, the calculated optical spectral bands and EPR parameters (Cal. IV) for $LiNbO_3$:Cu^{2+} are in agreement with the experimental values. Thus, the observed optical and EPR spectra for the Cu^{2+} center in $LiNbO_3$ are uniformly interpreted. This suggests that (i) the $[CuO_6]^{10-}$ octahedron in the trigonal $LiNbO_3$ crystal is indeed rhombic symmetry caused by the JT effect and (ii) the admixture of *d*-orbitals in the ground state for the impurity of the Cu^{2+} ion cannot be ignored.

1) The studied Cu^{2+} center in $LiNbO_3$ exhibits moderate covalency and impurity-ligand orbital admixtures, characterized by the relatively low covalency factor N (~0.83 < 1) and the significant orbital admixture coefficients λ_γ (~0.29–0.46) obtained from the cluster approach. Thus, the anisotropic contributions to the EPR parameters from the different components of the orbital reduction factors (with the relative deviation $k/k' - 1 \approx 33\%$) and the SOC coefficients (with the relative deviation $\zeta/\zeta' - 1 \approx 3.1\%$) should be taken into account using the cluster approach. When the ligand orbital and SOC contributions are neglected, the theoretical results (Cal. I) are not as good as those (Cal. IV) including these contributions (Table 1). Thus, the present perturbation formulas including the ligand orbital and SOC contributions are more reasonable in the studies of EPR parameters for d^9 ions in rhombic symmetry.

2) For copper in an octahedral environment under rhombic distortion, the ground state of the central Cu^{2+} is neither pure $^2A_{1g}(\theta)$ nor $2A_{1g}'(\varepsilon)$, but an admixture of both states. Table 1 shows that the calculated EPR parameters (Cal. IV), by applying the perturbation formulas and including the admixture between $^2A_{1g}(\theta)$ and $^2A_{1g}'(\varepsilon)$ states, are consistent with the experimental data and better than those neglecting the contributions from the admixture of the d-orbitals (i.e., Cal. II, $\alpha = 1$, $\beta = 0$). This means that the mixing coefficients α (and β) obtained in this work are suitable, although the admixture of $^2A_{1g}$ state into the ground state $^2A_{1g}'$ is insignificant (i.e., $\beta \approx 0.126$). Thus, the contributions to the EPR parameters due to this admixture cannot be ignored. Moreover, the mixing coefficient α (~0.992) for the present Cu^{2+} center is also in good agreement with that based on the analysis of the EPR parameters for the rhombic CuO_6 clusters in crystals [43–46].

3) From Eq. (4), one can find that the hyperfine structure constants originate mainly from the isotropic contributions proportional to the core polarization constant κ, characteristic of the Fermi contact between the ground 3*d*–3*s* (4*s*) orbital admixtures for the Cu^{2+} ion. In addition, the hyperfine structure constants A_i are related to the *g* shifts (i.e., $g_i - g_s$) as well as the average covalency factor N for the Cu^{2+} center. The signs of hyperfine structure constants A_i for the doped TM ions in crystals are difficult to ascertain from only the EPR experiments [26–28, 47–50]. However, our present calculations and the various observed values [22–26, 46, 50] reveal that the signs of A_x, A_y are positive, and A_z is negative. The negative sign of A_z can be illustrated by the larger magnitudes of the negative terms related to $(\kappa - 4N/7)$ than those of the positive terms related to the anisotropic contributions.

Conclusions. By analyzing the EPR parameters and optical spectral bands of the Cu^{2+} center in $LiNbO_3$, the local structure of the impurity of the Cu^{2+} is obtained, i.e., the rhombic octahedra $[CuO_6]^{10-}$ in $LiNbO_3$ crystal is found to exhibit the axial elongation $\delta z \approx 0.0611$ Å along *z*-axis and the planar bond length variation $\delta x \approx 0.0861$ Å along the *x*- and *y*-axes owing to the Jahn–Teller effect. Meanwhile, the ground-state wave function for the Cu^{2+} center in $LiNbO_3$ was also obtained. Generally, $LiNbO_3$ crystal has extensive applications in laser technologies and nonlinear optics, which strongly depends on the presence of defects caused by the transition metal impurities. Such impurities are responsible for modifications of the optical properties of crystals required for particular laser applications. In addition, the photorefractive effect, which is used for the storage of volume phase holograms, is also due to the presence of transition metal impurities (Fe, Cu, etc.) and intrinsic lattice defects. Therefore, it is of theoretical and practical significance to obtain the local structure for the Cu^{2+} center in $LiNbO_3$ crystal in this work.

Acknowledgements. This work was financially supported by the Foundation of Jiangxi Educational Committee (Grant No. GJJ211703) and Chinese Natural Science Foundation (Grant No. 11865013).

REFERENCES

1. T. P. J. Han, F. Jaque, *Opt. Mater.*, **29**, 1041–1043 (2007).
2. Ch. H. Kwak, G. Y. Kim, B. Javidi, *Opt. Commun*., **437**, 95–103 (2019).
3. L. Zhu, D. Zheng, S. Saeed, S. Wang, H. Liu, Y. Kong, S. Liu, S. Chen, L. T. Zhang, J. D. Xu, *Crystals*, **8**, 322, 1–8 (2018).
4. T. Tian, Y. F. Kong, S. G. Liu, W. Li, L. Wu, S. L. Chen, J. J. Xu, *Opt. Lett.*, **37**, 2679–2681 (2012).
5. L. Dai, Y. Shao, C. R. Liu, R. R. Chen, X. B. Han, S. X. Yang, *Opt. Mater.*, **95**, 109193 (2019).

6. A. V. Yatsenko, S. M. Kostritskii, *Tech. Phys.*, **65**, 622–626 (2020).
7. C. Xu, L. Xu, X. Leng, Y. Xu, C. Yang, *Cryst. Res. Tech*., **47**, 19–24 (2012).
8. N. V. Sidorov, M. N. Palatnikov, N. A. Teplyakova, R. A. Titov, K. Bormanis, *Integr. Ferroelectr.*, **196**, 39–42 (2019).
9. H. N. Dong, P. Li, *Spectrochim. Acta A*, **76**, 33–36 (2010).
10. R. Kripal, S. D. Pandey, *Physica B*, **444**, 14–20 (2014).
11. H. N. Dong, X. S. Liu, *Mol. Phys.*, **113**, 492–496 (2015).
12. M. Fidan, F. Semerci, E. Sahin, O. Z. Yesilel, R. Tapramaz, Y. Sahin, *Spectrochim. Acta A*, **110**, 437–442 (2013).
13. H. M. Zhang, W. B. Xiao, X. Wan, *Physica B*, **449**, 225–228 (2014).
14. R. Kripal, S. Shukla, *Phys. Scr.*, **83**, 035702, 1–6 (2011).
15. A. K. Yetrosyan, R. M. Khaghatryan, E. G. Sharoya, *Phys. Status Solidi b*, **122**, 725–734 (1984).
16. M. Q. Kuang, S. Y. Wu, H. M. Zhang, *Optik*, **123**, 1601–1604 (2012).
17. H. M. Zhang, W. B. Xiao, *J. Alloys Compd.*, **745**, 586–591 (2018).
18. A. M. Glass, *J. Chem. Phys*., **50**, 1501–1510 (1969).
19. L. Sun, J. Guo, R. Zhang, E. Cao, Y. Zhang, W. Hao, L. Ju, *J. Magn. Magn. Mater.*, **449**, 545–551 (2018).
20. K. Mukai, T. D. Inoue, Y. Kato, S. Shirai, *ACS Omega*, **2**, 864–872 (2017).
21. C. Wu, J. Zhong, J. Xie, D. Wang, Y. Shi, Q. Chen, H. Yan, J. Zhu, *Appl. Surf. Sci.*, **484**, 112–123 (2019).
22. H. M. Zhang, S. Y. Wu, M. Q. Kuang, Z. H. Zhang, *J. Phys. Chem. Solids*, **73**, 846–850 (2012).
23. A. S. Chakravarty, *Introduction to the Magnetic Properties of Solids*, Wiley Interscience Publ., New York (1980).
24. K. Küçük, Y. Çelik, R. Sahin, B. Karabulut, Ö. Andaç, N. Dege, *Chem. Phys. Lett*., **592**, 59–63 (2014).
25. E. Borkurt, I. Kartal, B. Karabulet, I. Ucar, *Spectrochim. Acta A*, **71**, 794–797 (2008).
26. H. M. Zhang, B. J. Chen, C. D. Feng, W. B. Xiao, *Appl. Magn. Res*., **50**, 1205–1217 (2019).
27. B. R. McGarvey, *J. Phys. Chem*., **71**, 51–66 (1967).
28. H. N. Dong, S. Y. Wu, P. Li, *Phys. Status Solidi b*, **241**, 1935–1938 (2004).
29. S. Y. Wu, X. Y. Gao, H. N. Dong, *J. Magn. Magn. Mater.*, **301**, 67–73 (2006).
30. J. S. Griffith, *The Theory of Transition-Metal Ions*, Cambridge University Press, London (1964).
31. D. J. Newman, B. Ng, *Rep. Prog. Phys*., **52**, 699–762 (1989).
32. H. M. Zhang, J. H. Duan, W. B. Xiao, X. Wan, *J. Non-Cryst. Solids*, **425**, 173–175 (2015).
33. C. C. Ding, X. H. Chu, L. Jia, X. Wang, Y. Li, Z. Q. Wang, J. Fu, *J. Non-Cryst. Solids*, **532**, 119896 (2020).
34. C. Rudowicz, Y. Y. Zhou, *J. Magn. Magn. Mater.*, **111**, 153–163 (1992).
35. H. N. Dong, *Z. Naturforschung A*, **60**, 615–618 (2005).
36. H. M. Zhang, *J. Magn. Magn. Mater*., **389**, 176–179 (2015).
37. Y. X. Hu, S. Y. Wu, X. F. Wang, *Philos. Mag.*, **90**, 1391–1400 (2010).
38. S. Y. Wu, H. M. Zhang, P. Xu, S. X. Zhang, *Spectrochim. Acta A*, **75**, 230–234 (2010).
39. K. H. Karlsson, T. Perander, *Chem. Scr*., **3**, 201–205 (1973).
40. C. K. Jorgensen, *Absorption Spectra and Chemical Bonding in Complexes*, 2nd ed., Pergamon Press, Oxford (1964).
41. E. Clementi, D. L. Raimondi, *J. Chem. Phys.*, **38**, 2686–2689 (1963).
42. E. Clementi, D. L. Raimondi, W. P. Reinhardt, *J. Chem. Ph*ys., **47**, 1300–1307 (1967).
43. E. Bozkurt, B. Karabulut, İ. Kartal, Y. S. Bozkurt, *Chem. Phys. Lett.*, **477**, 65–69 (2009).
44. I. Uçar, *Spectrochim. Acta A*, **72**, 399–406 (2009).
45. I. Uçar, B. Karabulut, A. Bulut, O. Büyükgüngör, *Spectrochim. Acta A*, **71**, 1239–1245 (2008).
46. H. M. Zhang, W. B. Xiao, X. Wan, *Radiat. Ef. Defects Solids*, **169**, 603–609 (2014).
47. C. C. Ding, S. Y. Wu, Q. S. Zhu, Z. H. Zhang, B. H. Teng, M. H. Wu, *J. Phys. Chem. Sol.*, **86**, 141–147 (2015).
48. H. M. Zhang, C. Yan, Q. S. Zhu, *Magn. Res. Chem.*, **57**, 144–148 (2019).
49. C. C. Ding, S. Y. Wu, X. F. Hu, G. L. Li, Y. Q. Xu, *J. Alloys Compd.*, **664**, 250–255 (2016).
50. Y. D. Li, B. J. Chen, C. Yan, H. M. Zhang, W. B. Xiao, *Radiat. Ef. Defects Solids*, **175**, 952–960 (2020).